Numerical simulation of the 3-D turbulent steady compressible flow in type "T" junctions and experimental validation of the total pressure loss coefficient

J. Pérez García, I. Murcia Murcia, J. Hernández Grau,
J. Martínez García and A. Viedma Robles.
Department of Thermal and Fluids Engineering
Technical University of Cartagena

ABSTRACT

Nowadays, simulation models of steady and transient compressible internal flow are essential in analyzing devices and plants where piping systems for gases and steam are required, such as, pneumatic fluid power systems, transport piping systems, inlet and exhaust systems in alternating combustion engines and compressors. Models used in the simulation of steady and transient compressible flow in junctions require local total pressure loss coefficients.

These coefficients can be experimentally obtained although a experimental support highly cost is required. Moreover, the internal flow behaviour is unknown. Alternatively, these coefficients can be obtained through numerical simulation using a 3D CFD general purpose software adequately validated.

This work is aimed to numerical simulation of 3D steady compressible flow at junctions "T" type. The geometrical characteristics and the different types of mesh used during simulations will be described, as well as numerical schemes, turbulence models, boundary conditions and more adequate simulation hypothesis.

The applied procedure to experimental validation of the numerical results for the total pressure loss coefficient in steady compressible flow in "T" type junctions will be presented. The experimental results were obtained in a flow bench for several combining and dividing flow configurations and for different mass flow ratios between branches as a function of local Mach number at intersection point in the common branch.

The comparison of numerical results with experimental and reference data, allow us selecting and adjusting simulation parameters, such as optimal turbulence model, boundary conditions, grid sensitivity and size, as well as most suitable adaption method in each case, discretization model and algorithm to solve the equations.
Keywords: *pneumatic junction, flow bench, compressible, steady, total pressure loss coeffcient, numerical simulation*

NOMENCLATURE

L_n	Branch length
A_n	Pipe area
K_{ud}	Total pressure loss coefficient (upstream, downstream)
p_{ou}	Upstream total pressure
p_{od}	Downstream total pressure
P_{0com}	Common branch total pressure
p_{com}	Common branch static pressure
D	Pipe diameter
M	Mach number
q	Mass flow ratio between N and G branches.

1 INTRODUCTION

The design process of pipe systems for fluid power pneumatic applications requires accurate predictions of the pipe system pressure loss. For a given pipe system, pressure losses sources can be described as friction in the pipes, bends, junctions, valves and other components. These predictions must be accomplished with low costs and short time at the development process. One way to solve this is to use one-dimensional code for pipe system modelling and introducing an empirical pressure loss coefficient into the code associated to each component. The characterization of the components with complicated geometry can be carried out in flow bench test or through numerical simulation by using 3D codes. The test in flow bench is very costly and only provides local total pressure coefficients. The numerical simulation shall be resolved within reasonable computational time and numerical procedures have to be validated with experimental reference data. 3D CFD simulations are useful in order to evaluate the flow behavior.

The empirical one dimensional model for the pressure loss coefficient is based on one of the three following assumptions. The first coefficient definition consists in supposing that there is a pressure drop between the inlet and outlet pipe because of the variation in the momentum. This pressure drop is defined by means of an expetimental coefficient, Benson (1975)[1], Binghan y Blair (1985)[2]. The second type of coefficient introduces an empirical equation in order to take into account the pressure drop (static or total) between the inlet and oulet, Dadone (1973)[3] y Morimune et al (1982)[4]. Lastly, the third type of coefficient consists on defining a discharge coefficent which establishes a relationship between actual mass flow rate and ideal mass flow rate assuming isentropic conditions for a singular element, Seifert y Schindler (1987)[5].

These coefficients have to be determined for each component and it is necessary to correlate these coefficients with the local Mach number.

The most realiable and complete experimental reference data for incompressible flow were obtained by Miller (1971, 1978) [6,7,8] as well as ESDU compilation (1973) [9,10]. The available information for compressible flow is limited, in open literature only data exists for 90º bends Ward-Smith (1964) [11] y ESDU [12], sudden changes in cross-sectional area Benedict (1980) [13], and some type of three-way junctions Abou-Haidar (1988)[14,15].

At the present time, through the raise of the computer power, CFD easily allows us to study flow in branched ducts. Most of the work has been focusing in design manifolds of ICE, and in all cases hypothesis of incompressible flow has been assumed. Fu et al (1992, 1994) [16,17] y Kuo y Chang (1993) [18] developed their own codes based on finite-volume for studying steady and incompressible flow between branches in two ducts manifolds. Leschziner y Dimitriadis (1989) [19] analyzed complex junctions such as pulse converter. Zhao y Winterbone (1994) [20] develoed in a code in order to solve flow through a manifold assuming incompressible flow. Other researchers used commercial codes such as STAR-CD or FLUENT/UNS for solving flow field in the interface plenum-runner in ICE manifolds Shaw et al (2000) [21]or for solving the whole inlet system.

However, there are no available data enough at open literature about total pressure loss coefficients in junctions for compressible flow. The preliminaires results of experimental and numerical research involving steady compressible flow in “T” type junctions will be presented in this paper. “T” type juctions are one of the most important component in

engineering. This element can be found in industrial applications like pneumatic fluid power systems, air transport systems, fluid devices y and manifolds at turbomachines.

This paper presents a numerical study which is part of the first stage of a combined experimental and numerical investigation of the internal compressible flow in the three-way junctions.

The global objetive is to validate a computacional metodology so as to obtain total pressure drop coefficients in steady compressible flow through adjusting simulation conditions and comparasion with experimental data obtained by mean of our flow bench and by reference. It will be possible to obtain correlations depending on Mach number and the mass flow rate between the ducts and for different type of flow both in joining and dividing flow, once the procedure has been validated. Finally, these empirical correlations could be implemented in one-dimensional codes, both steady and unsteady computation.

2 MATHEMATICAL MODEL

The RANS system equations for adiabatic steady compressible flow may be written in Cartesian tensor notation as:

$$\frac{\partial}{\partial x_i}\left(\rho u_i\right) = 0 \tag{1}$$

$$\frac{\partial}{\partial x_i}\left(\rho u_i u_j\right) = -\frac{\partial p}{\partial x_i} + \frac{\partial}{\partial x_j}\left[\mu\left(\frac{\partial u_i}{\partial x_j} + \frac{\partial u_j}{\partial x_i}\right) - \frac{2}{3}\delta_{ij}\frac{\partial u_l}{\partial x_l}\right] + \frac{\partial}{\partial x_j}\left(-\rho\overline{u_i' u_j'}\right) = -\frac{\partial p}{\partial x_i} + \frac{\partial}{\partial x_j}\bar{\tau}_{eff} \tag{2}$$

$$\frac{\partial}{\partial x_i}\left(u_i h_0\right) = \frac{\partial}{\partial x_j} u_i \bar{\tau}_{eff} \tag{3}$$

In order to model the Reynolds stress terms ($\overline{u_i' u_j'}$), different turbulence models can be used. In this simulation the standard, RNG and the realizable $k-\varepsilon$, the standard and the SST $k-\omega$, and the Spalart-Allmaras models were utilized. Also, the influence of the standard and non-equilibrium wall functions to simulate the near-wall region were tested. The second option generally provides better results than in most cases due to this last option uses wall laws for the mean velocity modified with the pressure gradient.

The Spalart-Allmaras turbulence model is the the simplest in mathematical terms. It is only one equation model and can be utilised in solving compressible flow involving soft recirculation zones and low intensity separation. It also can be used for boundary layers with adverse pressure gradients and wall- bounded flows.

The $k-\varepsilon$ realizable turbulence model has shown better performance for the simulated flow since it was designed in order to simulate internal flows in duct involving detachment. This model enforce some mathematical restrictions in normal stresses which gives good results at high Reynolds number flows.

Finally, the $k-\omega$ SST turbulence model is recommended both in compressible and incompressible low Reynolds number ($\mathrm{Re} < 1.10^6$).

3 GEOMETRY, FLOW TYPES IN JUNCTIONS AND MASS FLOW RATIO BETWEEN BRANCHES

Junctions can be classified according to geometry of 2D and 3D junctions. Moreover, both cases can deal with three or more branches. Three-way juntions can be T-type, in which place two of the three centerlines are aligned or Y-type, which can be symmetrical or non-symmetrical. On the whole, symmetry axes of each branch may not intersect at a certain point. In this paper, we will focus on junctions whose symmety axes intersect at the same point.

Next picture reveals the different flow types in a T-type junction that have been studied. The branch denominated "G" is allways the common branch, both in joining and dividing flows. The others branch are named "A" and "N". The mass flow ratio between branches is defined as $q = \dot{m}_N / \dot{m}_G$.

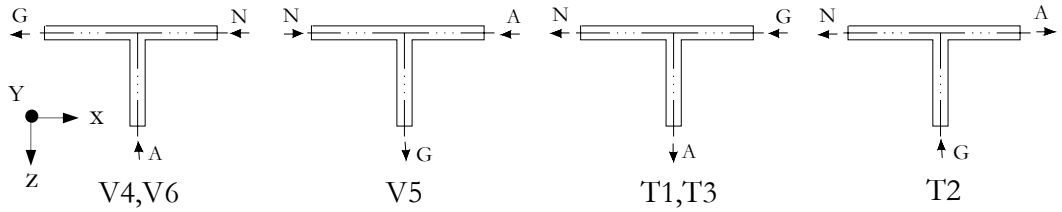

Picture 1. Flow configurations simulated in type "T" junctions

The junctions which are most interesting at industry are Y-type and T-type. Each geometry has been characterized for joining and dividing flows. The number of different flow types are $2^n - 2$, where *n* is the number of branches.

3.1 TOTAL PRESSURE LOSS COEFFICIENT DEFINITION

The pressure losses in junctions are caused by several factors, mainly: friction stresses due to flow viscosity, sudden flow direction and/or section changes which give arises to boundary layer separation and a section reduction effect, called "vena contracta", that may result in a pipe blockage, momentum transport and deformation between joining flows, or expanion and non-isentropic stagnation dividing flows.

There are several definitions for the total pressure loss coefficient depending on wheter the problem set up involves incompressible [6], or compressible flow [14]. In this paper, a pressure loss coefficient based on mechanical energy equation defined by Abou-Haidar [14] is utilized.

4 COMPUTATIONAL FLUID DYNAMIC 3D MODEL

The studied computacional domain is a three-way 90º T-junction with circular cross-sectional area consisting in a main straight duct connected to another sided one in 90º connection and also with the same cross-sectional area.

The suitability of working with a structured or non-structured mesh has been analyzed through a two dimensional mesh as well as the convenience of adapting at the zone adjacent to the walls. These two dimensional meshes were used due to their lower computational time needed.

4.1 NUMERICAL APROXIMATION

4.1.1 MESH

The internal flow behaviour at junction presents a very different characteristic depending of flow configuration and mass flow rate between branches. In the main flow analyzed cases,

both, combining and dividing flows, and for medium mass flow rates simulated, good results with a structured mesh have been obtained. Nevertheless, in several flow cases in dividing flows or when low mass flow rates are simulated, convergence problems have appeared. This may be caused by the hard curvature of stream lines. In this way, a non-structured mesh has been built. With this mesh, the time consumption is very high, which makes this option unfeasible.

A mesh composed by 300000 tetrahedral cells is needed in order to get the same results tas when using a structured mesh with 60000 hexahedral cells.

Numerical errors have been found in the flow simulations caused by a mathemathical indetermination.This is caused by the sharp edge located in the intersection region. A bevel edge to minimize this numerical error has been defined. The size of the chamfer is two wall cells, which is the same asusing a rounded edge of $r/D = 0.02$. Through this bevel edge numerical errors are reduced and there is no reduction on the total pressure loss coefficient..

4.1.2 BRANCH LENGTHS

The length of each branch is given in terms of the ratio L/D. The required length depends on: mass flow ratio between branches, flow type and more importanly on the mass flow rate in the common branch. For each flow type, the fluid domain can be optimized to reduce the compuational time, although, it would involve a generation of a specific geometry for each case.

In the main of simulated flow types, a ratio $L/D = 45$ has been utilized for all branches. The uniform flow condition has been tested in the most critical case and maximum mass flow rate at the common branch. In addition, in order to get a developed velocity profile after boundary condition “mass flow inlet” at most, a length $L/D = 15$ is needed.

4.1.3 Y^+

The wall-treatment laws for turbulent boundary layer implemented on Fluent are only valid in a specified y^+ range. This range fixes the distance from the centroid of the first cell to the wall. One has to do mesh sensibility research in order to optimize computation time. The computation time must be minimized but the numerical results have to be insensitive to the used mesh. For this reason, several cases have been computed using differents adaptions.In this way, as a criterium, a minimum value of $y^+ \approx 25$ has been adopted. The total pressure loss coefficient in this parametric study has been evaluated. This value of y^+ impose a minimum usable value of mass flow rate because when mass flow rate decrease, y^+ also does.

On the other hand, maximum mass flow rate is also fixed by the boundary conditions. “Mass flow intlet” is a rigid boundary condition and a chocked effect caused by the friction may appear due to the required length of each branch. Fluent is not able to recognize this physical effect and the mass flow rate is not set correctly because this would involve changing in the previous fixed value of the boundary condition.

Summing up, in the final mesh, a ratio $y/D = 0.07$ from the centroid of first cell to the wall is used. The minimum value of y^+ enforces a minimum value of the mass flow rate arround 0.02 Kg/s. On the other hand, friction effect imposes a maximum value in the mass flow rate of 0.08 Kg/s. Working on this mass flow rate range, it is possible to simulate junctions in a Mach number range of $0.2 \le M_{com} \le 0.6$. If lower Mach number is required, it

is necessary to build another mesh. This mesh should be coarsen at the walls or shorther branches should be made. However, this last solution will affect to the velocity profile uniformity.

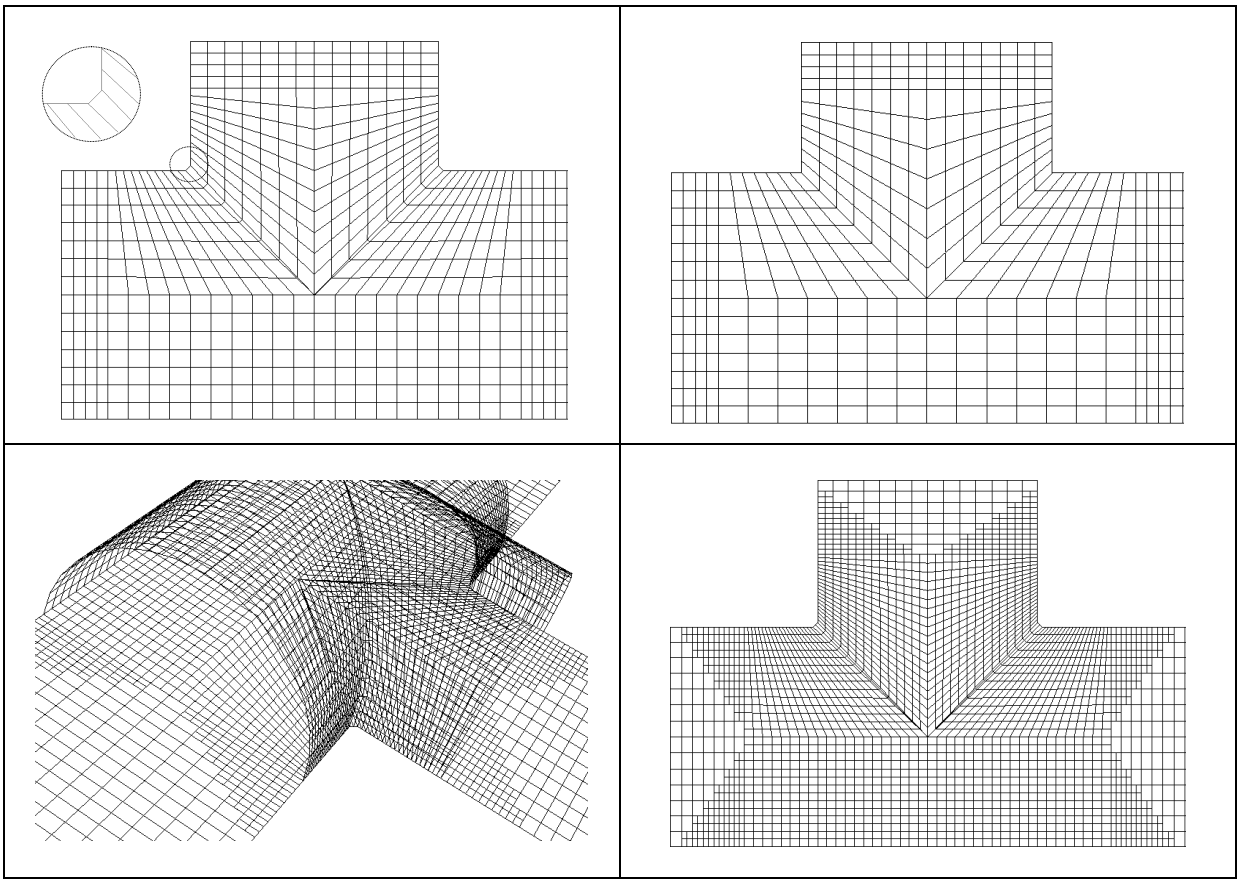

Picture 2. Meshing the junction

4.2 SOLVER

In high-medium compressible flow the coupled solver is recommended, however, in low compressible flow the segregated solver can provide adequate results with a lower computational cost.

In the figures 1 and 2, the total pressure loss coefficient K_{AG} and K_{GN} in joining V4 flow type with a mass flow ratio of $q = 0.5$, by using the segregated and coupled solver are compared versus reference data. The same turbulence model has been used in both cases has been use (the realizable $k - \varepsilon$). It can be seen that coupled solver numerical results overestimates arround 5% and 10% to the segregated solver. Moreover, it is noticeable that the computation time is extremely high when coupled solver is utilized.

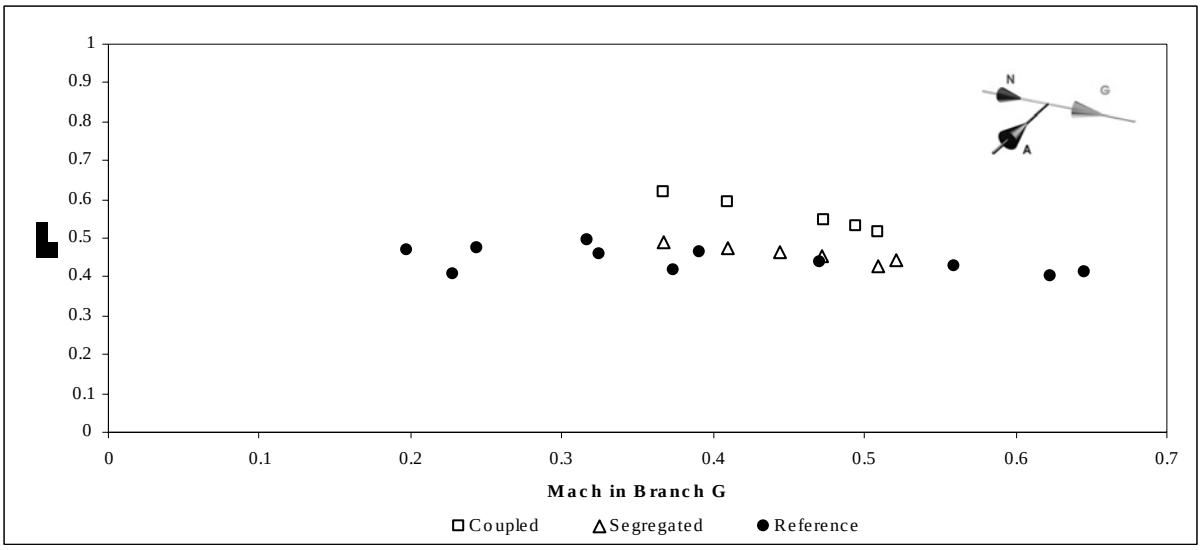

Figure 1. K_{AG} total pressure loss coefficient in coupled and segregated solver.

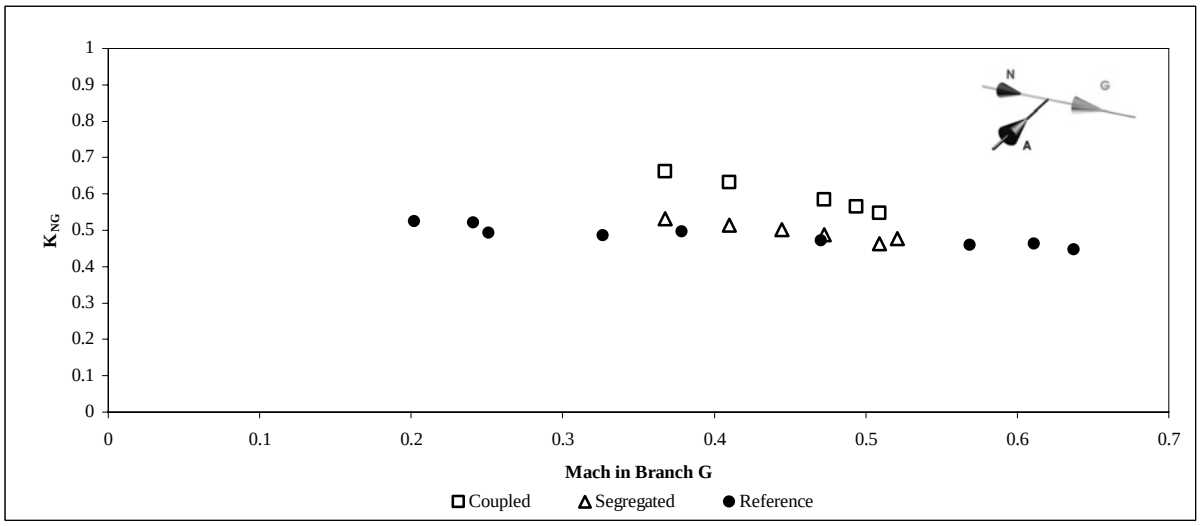

Figure 2. K_{AN} total pressure loss coefficient in coupled and segregated solver.

Due to the higher compuational time required by coupled solver (up to 15 times more) and to the fact that most of the studied cases are in the range of the medium-low compressible flow, the segregated solver is used. The remaining options that have been selected were: second-order discretization scheme, SIMPLE pressure-velocity coupling and implicit algorithms.

4.3 BOUNDARY CONDITIONS

Fluent provides several types of boundary conditions for the specification of flow inlets and outlets. Selecting boundary conditions depends on the characteristics of the simulated flow. In this paper, four differents boundary conditions have been employed. Simulating joining flow cases, two branches are in inlet and one is in outlet (common branch). The most suitable boundary condition at inlet is "mass flow inlet" and at outlet (common) "pressure outlet" due to total pressure loss coeficient have to be obtained for a fixed mass flow ratio.

If the a dividing flow case is being simulated, the most suitable boundary conditions are "mass flow inlet" in the common branch and "pressure outlet" at the outflow branches.

Nevertheless, as mass flow ratio have to be fixed by user, it is necessary deactivate one pressure outlet boundary in order to fix the mass flow rate there, instead of fixing the pressure. It is necessary to enable the option "target-mass-flow-rate-settings" on this boundary to achieve this goal.

In order to reduce the computation time, half a domain has been simulated. Because of that, symmetry boundary condition has to be imposed at the plane ZX.

An the wall boundary condition, the roughness of the wall, the adiabatic flow hypothesis and no-slip conditions have to be specified. Roughness is really important at solution due to the required lengh at the branches. In all studied cases, absolute roughness value adopted was set to $k = 7.5.10^{-6}\ m$ and a roughness constant of 0.5. This parameter is also fixed in the post-procesing code with the purpose of discounting the pressure drop caused by friction and extrapolating flow variables to the flow crossing.

4.4 TURBULENCE MODELS

It is well known that no single turbulence model is universally accepted as being superior for all kinds of problems. The choice of turbulence model will depend on several considerations such as the physics of the flow, the established practice for a specific sorts of problem, the accuracy level required, the available computational resources, and the amount of time available for the simulation.

Most of the research work used the standard $k-\varepsilon$ turbulence model. In this paper, a parametrical study with all the RANS turbulence models implemented in Fluent, which are needed to achieve "closure" the Reynolds-averaged Navier-Stokes (RANS) equations, has been accomplished. The Reynolds-averaged approach is generally adopted for practical engineering calculations, and uses models such as the Spalart-Allmaras, the $k-\varepsilon$ and its variants, the $k-\varpi$ and its variants, and the RSM.

There are differences among the results for each turbulence models and these are significant in some flow types. The next figure depictes the value of the total pressure loss coefficient obtained in a V4 joining flow type, mass flow ratio of $q = 0.5$ and mass flow rate at common branch of 0.08 Kg/s. The tested RANS turbulence models are: the RSM, the $k-\varpi$ standard and SST, the $k-\varepsilon$ standard and realizable with non-equilibrium wall functions, and Spalart-Allmaras with the vorticity-based production option.

Thus, the total pressure loss coeffient is represented for different values of L/D ratio. It can be seen that all turbulence models predict the same total pressure loss coefficient accurately and there are not notable differences among any of the tubulence models.

The figures 3 and 4 show the value of the total pressure loss coefficients obtained in a V4 joining flow type, mass flow ratio of $q = 0.5$ in a Mach number range. The three turbulence models correctly predict the same tendency and the realizable $k-\varepsilon$ fits better with the reference experimental data. Using the SST $k-\varpi$ model, differences are outsized, while Spalart-Allmaras model shows a intermediate performance.

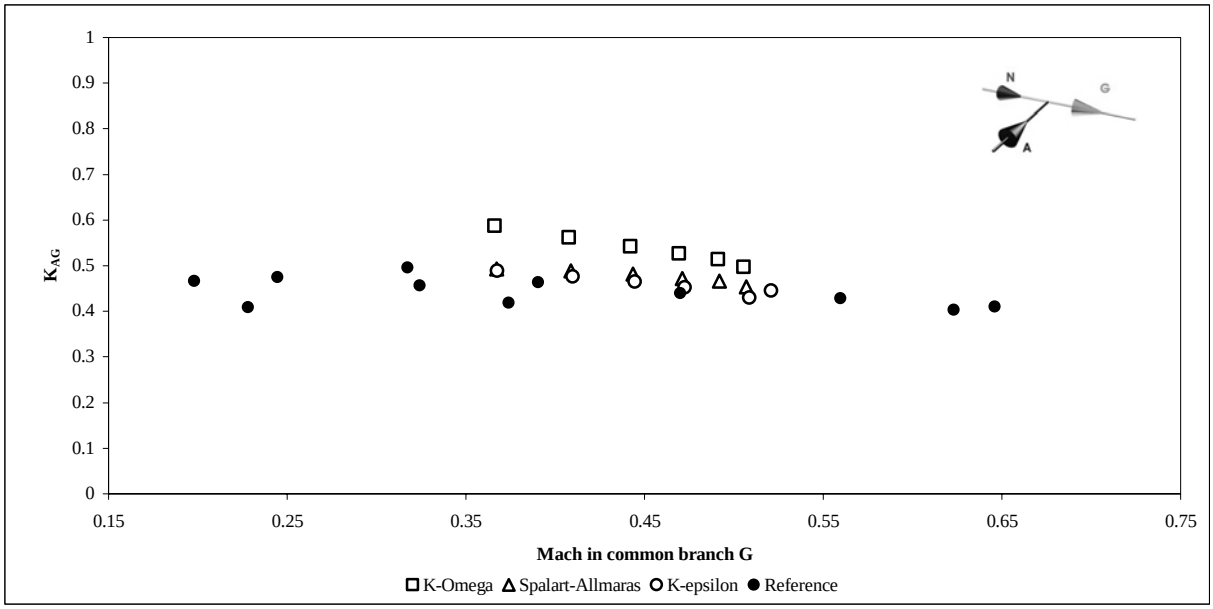

Figure 3. K_{AG} total pressure loss coefficient in several turbulence models

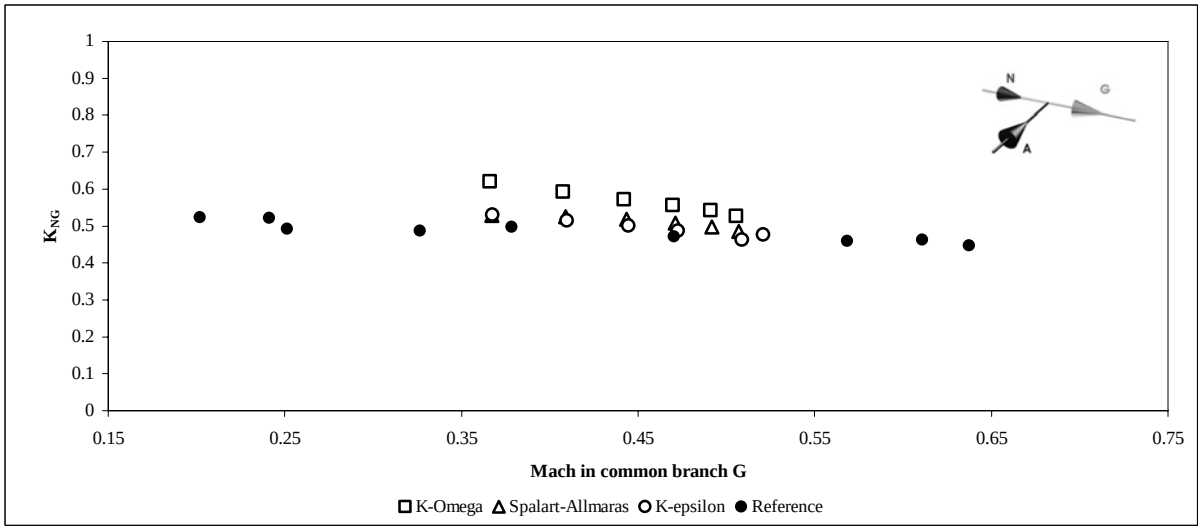

Figure 4. K_{NG} total pressure loss coefficient in several turbulence models.

A comparation between the standard and the non-equilibrium wall function for all RANS turbulence models have been accomplished. This comparation was made in a V4 flow type, $q = 0.5$ and mass flow rate at "G" branch of 0.08 Kg/s. Thus, Mach number value at these cases is 0.52. Negligible differences between the standard and non-equilibrium wall funtions have been found. By consequent, in all cases, non-equilibrium wall functions will be used.

5 NUMERICAL RESULTS PROCESSING METHODOLOGY

A computational methodology has been developed to predict the total pressure loss coefficient in compressible internal flow in three-way junctions.

For all combining and dividing converged cases, by means of simulation software Fluent, a journal file is runed. This journal creates several iso-surfaces along the three

branches and computes results of mass flow rate, mean static pressure and temperature in each section.

The figure 5 shows a typical variation of the mean total pressure along straight pipe lengths in a 90º T-junction. In this case, the influence of the junction extends up to about *15D* upstream and up to *35D* downstream. In order to determine the pressure losses just at the junction, the friction losses are not included within the coefficient calculation.

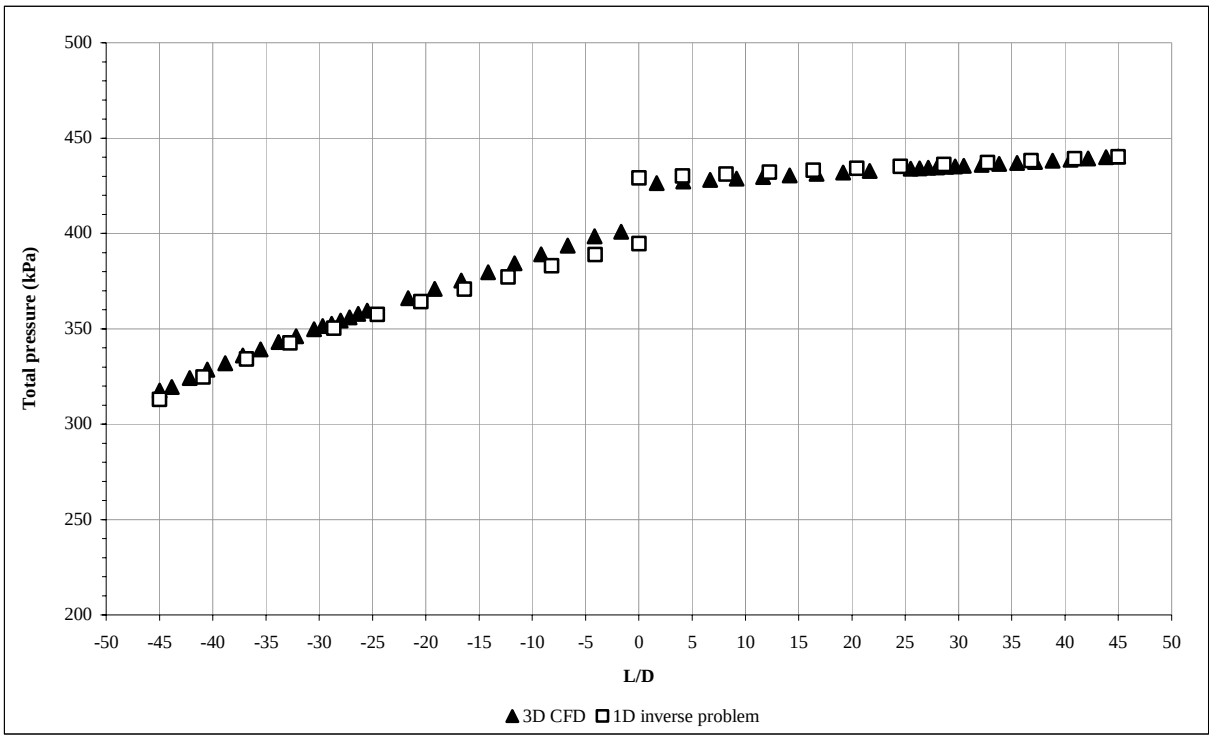

Figure 5. Total pressure predicted and extrapolated in branches A and G for a V4 joining flow type

Assuming one-dimensional adiabatic friction flow, it is possible to obtain an analytical solution [24] to extrapolate the total pressure determined to a especified location, measured until the intersection of the junction-pipes in centerline-axis. The extrapolated flow properties are obtained through upstream and downstream calculations depending of flow direction in each branch. The input data are the mass flow rate, and the mean static pressure and temperature in each section evaluated departing from numerical results obtained by Fluent, and the non-dimensional roughness. This coefficient is experimentally determined in flow bench or numerically [25]. The obtained value is also used in the numerical simulation by Fluent.

The extrapolation procedure is accomplished for different values of ratio L/D and respective total pressure loss coefficient is calculated. The defined calculation procedure has been implemented in a Mathematica® notebook [26].

$$K_{u,d} = \frac{p_{0,u} - p_{0,d}}{p_{0,com} - p_{com}} \tag{4}$$

Departing from similar plots to the figure 6, an interval of $25 < L/D < 35$ in order to evaluate the total pressure loss coefficient has been established. Inside this interval fully-developed flow is achieved and fluid properties are approximately uniform.

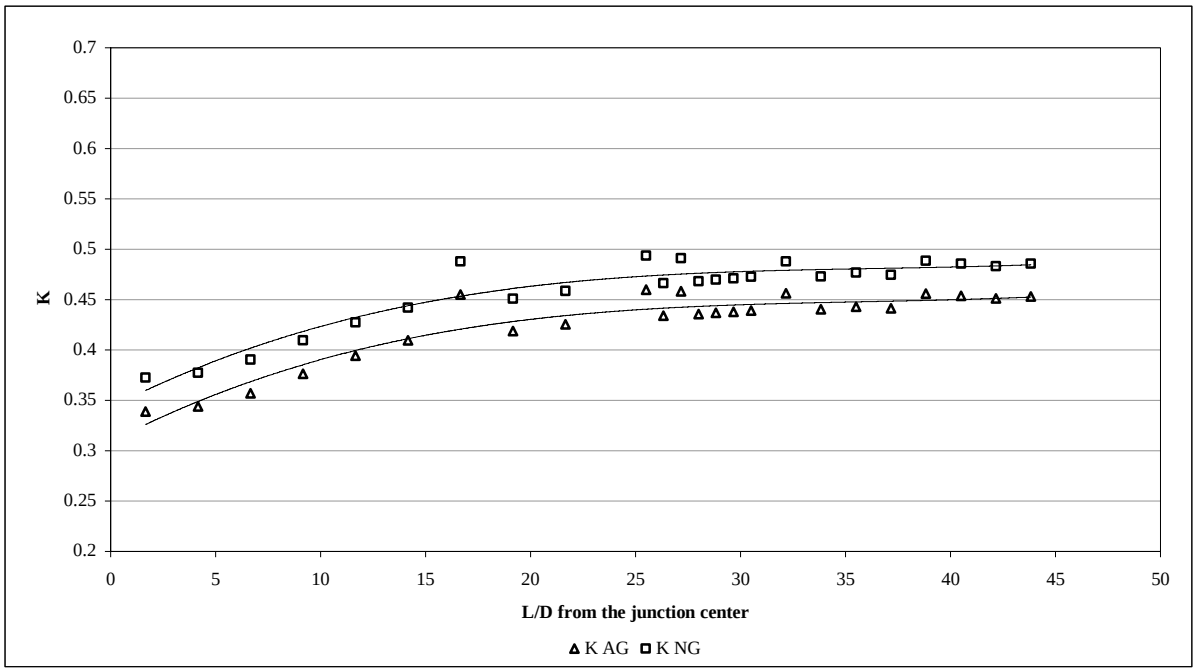

Figure 6. Total pressure loss coeficient calculated for different L/D ratios in straight pipe upstream and downstream at the junction, K_{AG} and K_{NG},, q=0.5, V4 flow type, mG=0.08 Kg/s

6 RESULTS. VALIDATION AND DISCUSSION

6.1 REFERENCE DATA

The reference data about steady compressible flow in three-way juntions are avaliable in [14, 15]. These data concern total pressure loss coefficient between one sided branch and the common one at different mass flow ratios (0, 0.25, 0.5, 0.75 and 1) and for interval Mach number which oscilates between 0.2 and 0.6. In this reference data, a "T" junction is studied with different angles between its branches (30º, 45º, 60º y 90) with sharp edge and without area changes.

6.2 EXPERIMENTAL DATA

6.2.1 EXPERIMENTAL SETUP

The tests have been accomplished in a flow bench. The flow bench consists in a 36,8 kW screw compressor, which gives 400 Kg/h of mass flow rate at 8 bar, a reservoir of 1,5 m^3, and a cleaning system for the compressed air which is composed of a dryer, filtering line and a pressure regulator.

There are four parallel ducts to replicate of any flow type. Two Coriolis effect mass flow meters are instaled in order to be able to simulate the several diferent flow types in a three-way junction. These mass flow meters have an user defined range and are highly accurate. Others technical characteristics are indicated in [27].

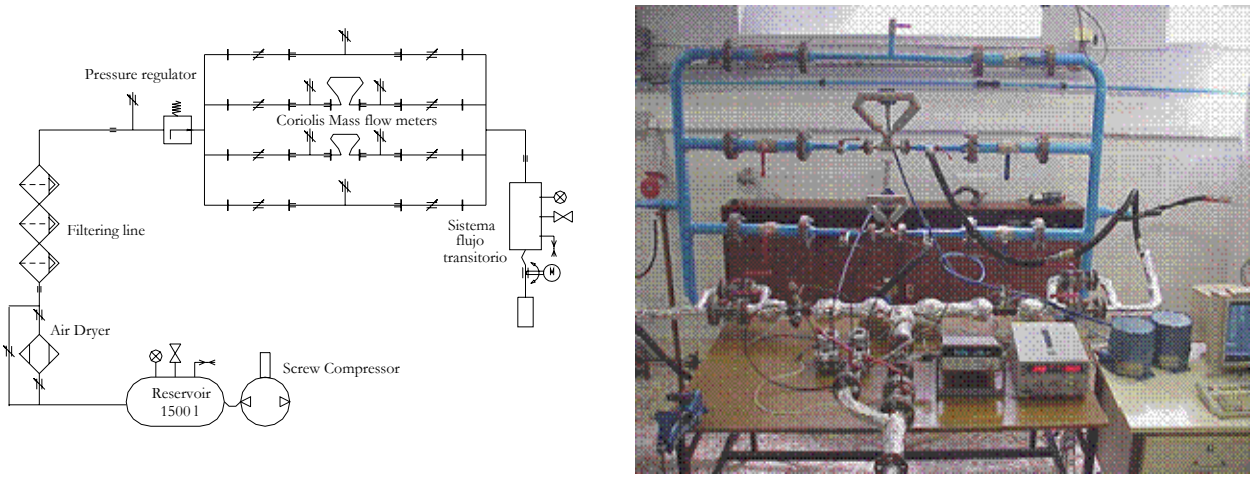

a) b)

Picture 3: a) Bench flow scheme b) Bench flow instrumentation

The tested 90º T-junction is circular cross-sectional area. All branches are 12 mm diameter with coplanar axis and sharp edge intersections. A flow straightener followed by an area reducing duct well upstream of the junction ensuring that the flow entering at the test section was fairly uniform. The absolute static pressure and static temperature are measured in a specific location in each branch. The static pressure drop is measured between each test section. Moreover, the mass flow rate is measured at two branches upstream at junction.

A straight length of *10D* separate the area reducer and the first measurement point. The test section is located at 30*D* from the junction centreline-axis.

The mean static pressure is measured with a extensiometric transmitter and the temperature by means a type-T thermocouple. The static pressure drop between common branch and other branch is measured by means of a differential piezo-resistive pressure transmitter. The measuring instrumentation system configuration is showed in picture 4.

A digital multimeter HP 34970A connected to PC by means RS-232 enables readings of mass flow meters, absolute and differential pressure transmitters and thermocouples. A software provides a txt-file with the readings. Starting from this file, a Mathematica® notebook accomplish the required calculation in order to reduce the data to the required form.

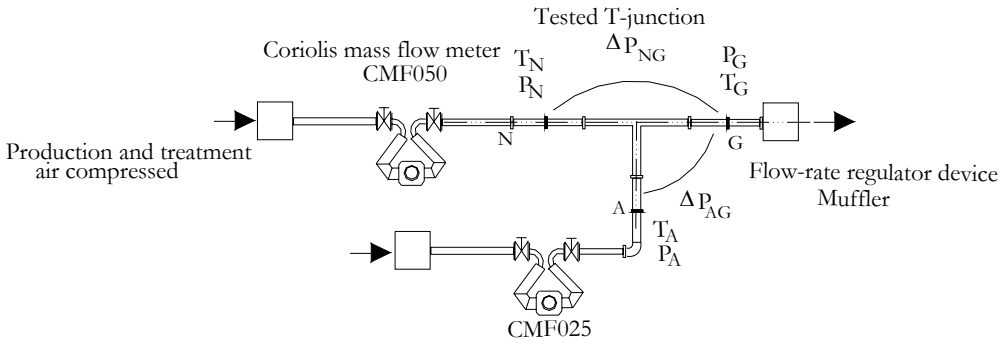

Picture 4. Measuring instrumentation system in junction tests

6.2.2 PROCESSING METHODOLOGY

The test procedure consist on following steps:

- Assembling the junction and adjusting , configuration and calibration of measurement system
- Establishing the different flow types which are going to be tested
- Fixing the mass flow ratio 0, 0.2, 0.25, 0.4, 0.5, 0.6, 0.75, 0.8 or 1
- Measuring static pressure and temperature, mass flow rate and static pressure drop keeping the same mass flow ratio and changing Mach number at the common branch (regulation valve downstream)
- Data processing and reducing. Data processing is based on the next steps:

a) Previous data treatment. Out coming files from the flow bench are modified in such a way that they are valid for the treatment data code
b) Introducing data input in the treatment software: L/D ratio, configuration files, geometrical data, file data number and name,…etc
c) Converting readings to physical units, raw data statistical treatment and flow properties and non-dimensional parameters calculation
d) Checking data consistence, plotting the corrected mass flow rate versus pressure ratio at junction

$$\dot{m}_G^* = \frac{\dot{m}_G}{A_G\, p_{o,u}} \sqrt{R_g T_{o,u}} \;\propto\; p_d / p_{o,u} \tag{5}$$

e) Calculating mass flow ratio and total pressure loss coefficients. It is possible to choose among different definitions for the total pressure loss coefficient. In his way, in a three-way junction, two coefficients are obtained, K_{GA} y K_{GN}. Different mass flow ratios and permissible errors can also be plotted
f) Results data file generation and graphical output. The final results are imported by Excel in order to compare with experimental reference data. Output graphics can be set up to plotting total pressure loss coefficient against different parameters such as Mach number, Reynolds number, pressure ratio,…etc

6.2.3 UNCERTAINTY OF MEASUREMENT

Experimental determination of the pressure loss coefficient as a function of mass flow ratio and Mach number in common branch entails an uncertainty due to measurements errors and their propagation in results. In the following tables, 1 and 2, results of uncertainty calculation under ISO standard "*Guide to the Expression of Uncertainty in Measurement*" [28] are showed.

Expanded Uncertainty (Confidence interval 95%)		
Temperature	*K*	*%*
Type T Thermocouple	*± 3.4*	*± 1.2*
Mass flow rate	*Kg/h*	*%*
CMF050 (Range 0-250 Kg/h)	*± 0.9*	*± 0.7*
Differential pressure	*mbar*	*%*
SMAR D2 (Range 0-500 mbar)	*± 0.6*	*± 0.12*
SMAR D3(Range (0-2500 mbar)	*± 2.4*	*± 0.1*
Absolute pressure	*bar*	*%*
CERALINE (Range 0-5 bar)	*± 0.03*	*± 0.6*

Table 1. Expanded uncertainty in measured quantities

Uncertainty propagation in results	
Mass flow ratio between branches ($q = \dot{m}_x / \dot{m}_{common}$)	± 1.2 %
Mach number ($M = \sqrt{\gamma R_g T}$)	± 0.5 %
Total pressure loss coefficient (K_{ud})	± 2.5 %

Table 2. Uncertainty propagation in results

6.3 RESULTS

6.3.1 FLOW STRUCTURE IN A 90º JUNCTION

Pictures 5 to 8 show the structure flow for V4 and V5 joining flow types and T1 and T2 dividing flow types. The contours of total pressure, density and Mach number and the velocity vectors in differents sections along to the pipes are depicted at the symmetry plane at T-junction.

In V4 flow type, joining flows a “vena contracta” effect which could to cause a chocked flow is observed. The density and Mach contours permit to observe that higher gradient area is located at the junction intersection edge between G and A branches. The velocity vectors representation allow us to identifie the branch length duct where the effective local junction effect takes importance.

The V5 flow type is a very complex case. In this flow type the vertical duct correspond to the common branch. Two separation and recirculation zones are generated in the common branch. A high velocity zone downstream junction can be seen. The fluid properties are uniformized in a sorther distance due to the flow symmetry.

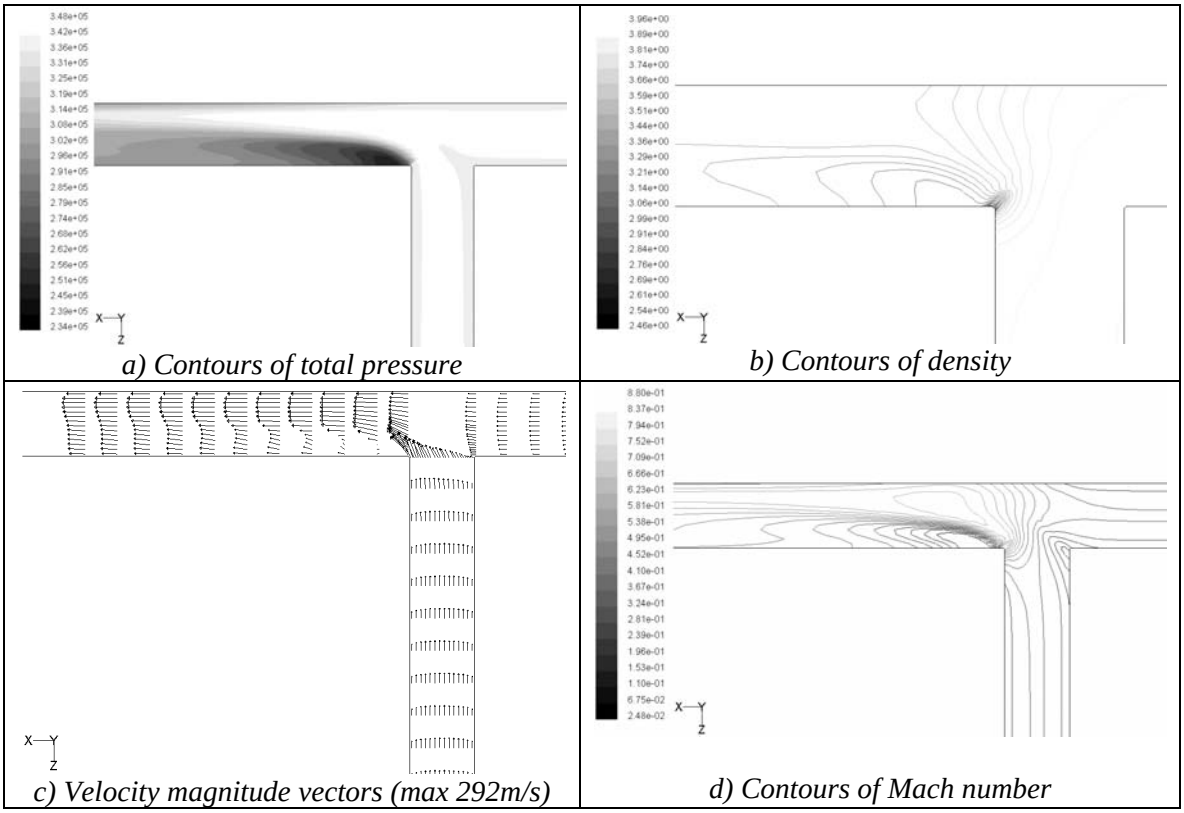

a) Contours of total pressure

b) Contours of density

c) Velocity magnitude vectors (max 292m/s)

d) Contours of Mach number

Picture 5. Total pressure, density, Mach number and velocity magnitude vectors in a V4 flow type, q=0.5, mG=0.06 Kg/s, at the symmetry plane

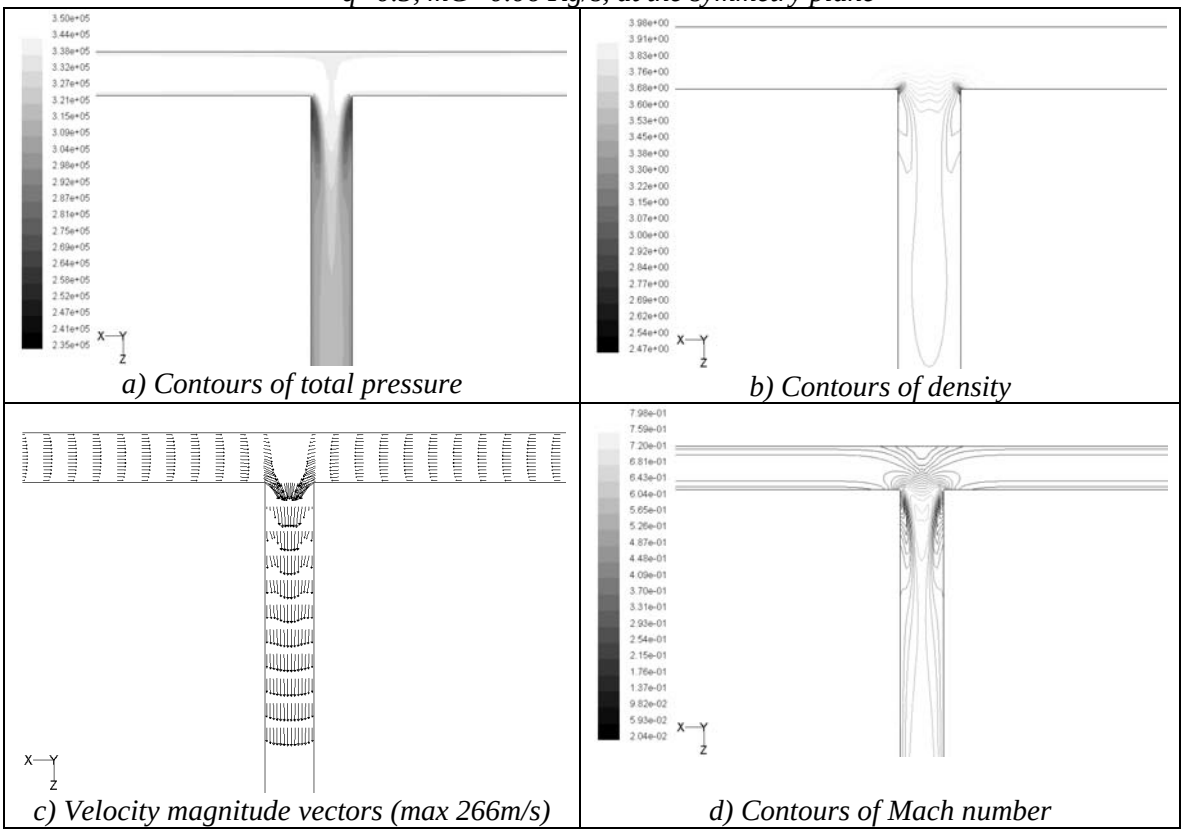

a) Contours of total pressure

b) Contours of density

c) Velocity magnitude vectors (max 266m/s)

d) Contours of Mach number

Picture 6. Total pressure, density, Mach number and velocity magnitude vectors in a V5 flow type, q=0.5, mG=0.06 Kg/s, at the symmetry plane

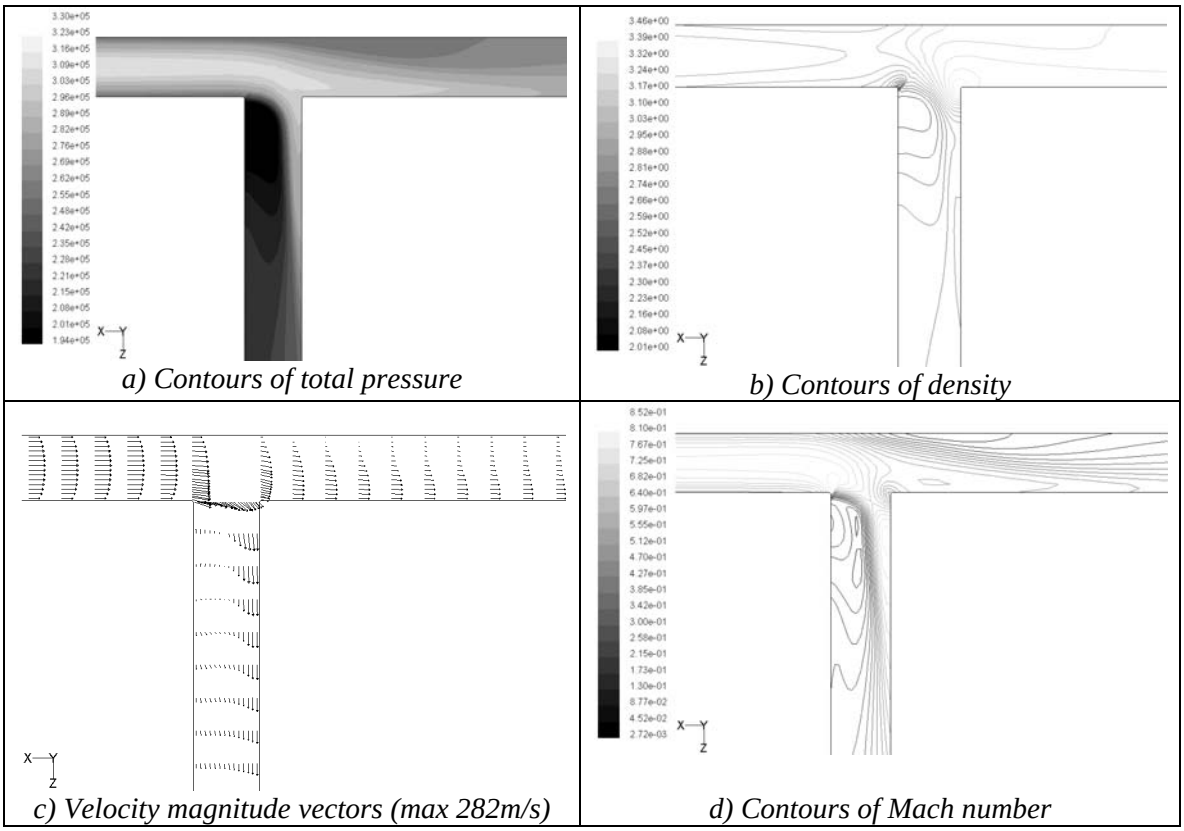

a) Contours of total pressure

b) Contours of density

c) Velocity magnitude vectors (max 282m/s)

d) Contours of Mach number

Picture 7. Total pressure, density, Mach number and velocity magnitude vectors in a T1 flow type, q=0.5, mG=0.06 Kg/s, at the symmetry plane

In T1 dividing flow type, the flow expandes giving arise to two large separation regions, one at the common branch and another at straight duct. Velocity vectors show the accentuate asymmetry at the velocity profiles.

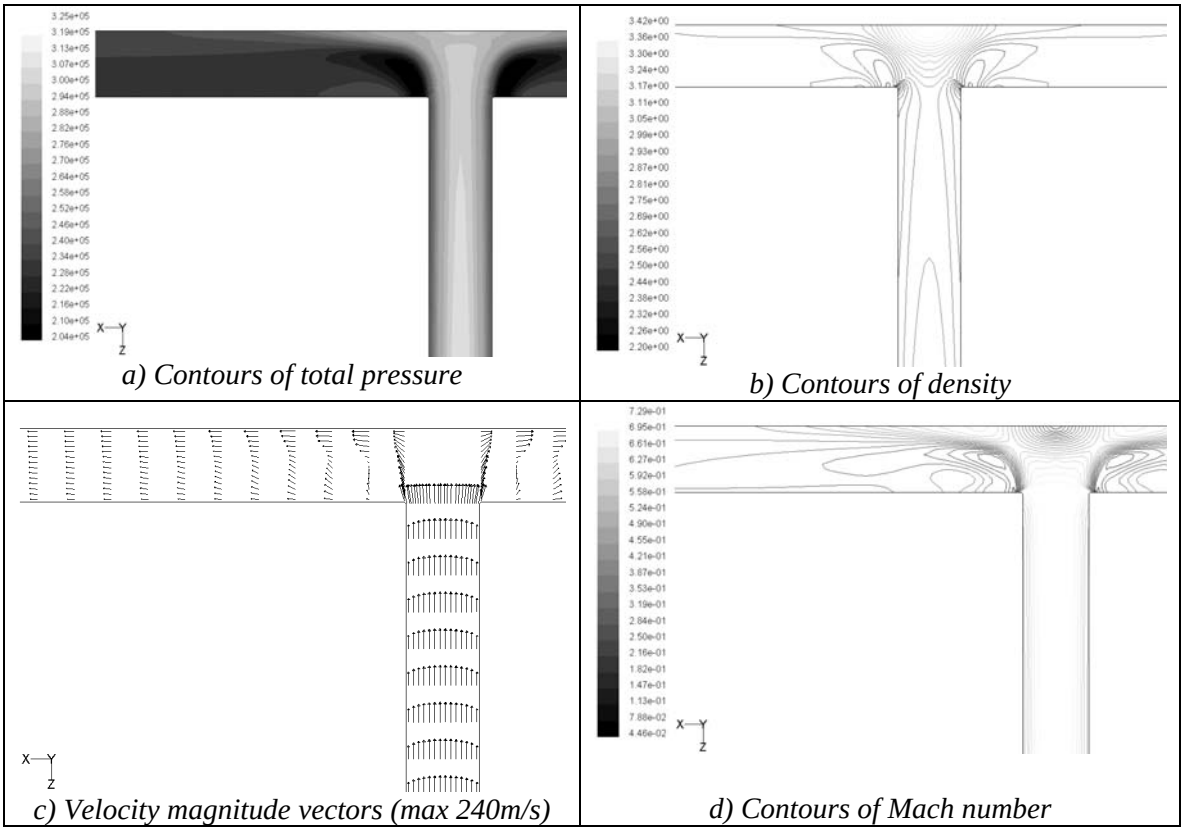

a) Contours of total pressure

b) Contours of density

c) Velocity magnitude vectors (max 240m/s)

d) Contours of Mach number

Picture 8. Total pressure, density, Mach number and velocity magnitude vectors in a T2 flow type, q=0.5, mG=0.06 Kg/s, at the symmetry plane e.

In T2 flow type, a great separation regions at the straigh branch it is observed. There is a large stagnation zone when the flow impinge on the front wall in straight duct, however, velocity profiles are fully-developed at the outlet sections in a short length.

6.4 COMPARISON AMONG NUMERICAL RESULTS, EXPERIMENTAL OWN DATA AND REFERENCE DATA FOR V4 FLOW TYPE

The next figures shows the total pressure loss coeficients K_{AG} and K_{NG} versus extrapolated Mach number in common branch to the junction centerline-axis.

6.4.1 COMPARISON BETWEEN NUMERICAL RESULTS AND REFERENCE DATA FOR V4 FLOW TYPE

Figures 7 and 8 show an excellent agreement among numerical results and reference and experimental data for a mass flow ratio of $q = \dot{m}_N / \dot{m}_G = 0.5$ in a V4 flow type.

There are a good agreement between experimental and the reference data for a mass flow ratio $q = 1$, but the numerical results are overtestimated. To the mass flow ratio $q = 0$, good concordance is obtained at low Mach number, however, when Mach number increases the difference grows up too. As to numerical results, there is a good agreement with our

experimental data at $q = 0$ and $q = 0.5$ while with $q = 1$ there is a qualitative agreement but not quantitative. This may be caused by our numerical methodology does not correctly predict the suction effect which appears on this case.

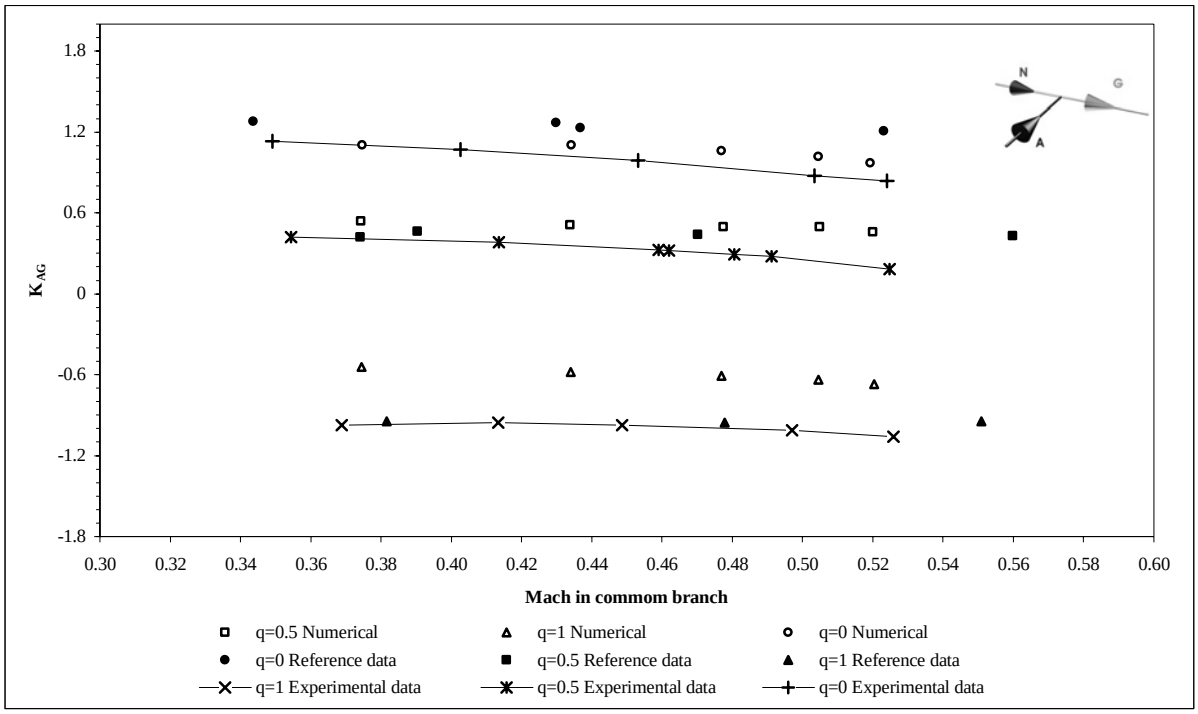

Figure 7. Coefficient K_{AG} with realizable k-ε non-equilibrium turbulence model in a V4 flow type

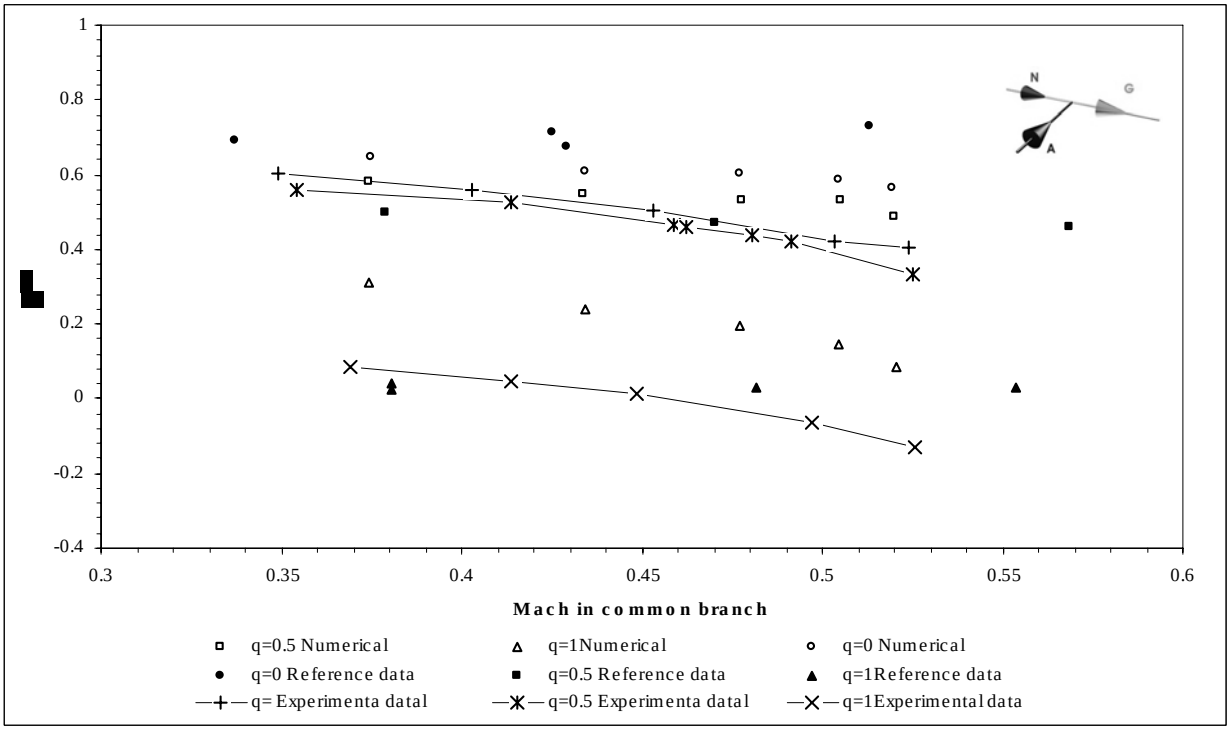

Figure 8. Coefficient K_{NG} with realizable k-ε non-equilibrium turbulence model in a V4 flow type

.

In the other hand, for the K_{NG} coefficient, a good agreement for $q = 0.5$ and $q = 0$ has been obtained, mainly at low Mach number.At high Mach number the numerical results are underestimated. For $q = 1$, non-significative differences appear between our experimental data and the reference data for low Mach number, differences are higher when Mach number increases. The numerical results in this mass flow rate are overestimated.

In general, there are a good agreement between numerical an our experimental data, although for $q = 1$ the same problem that in K_{AG} coefficient is revealed.

6.4.2 COMPARISON BETWEEN NUMERICAL RESULTS AND REFERENCE DATA FOR V5 FLOW TYPE

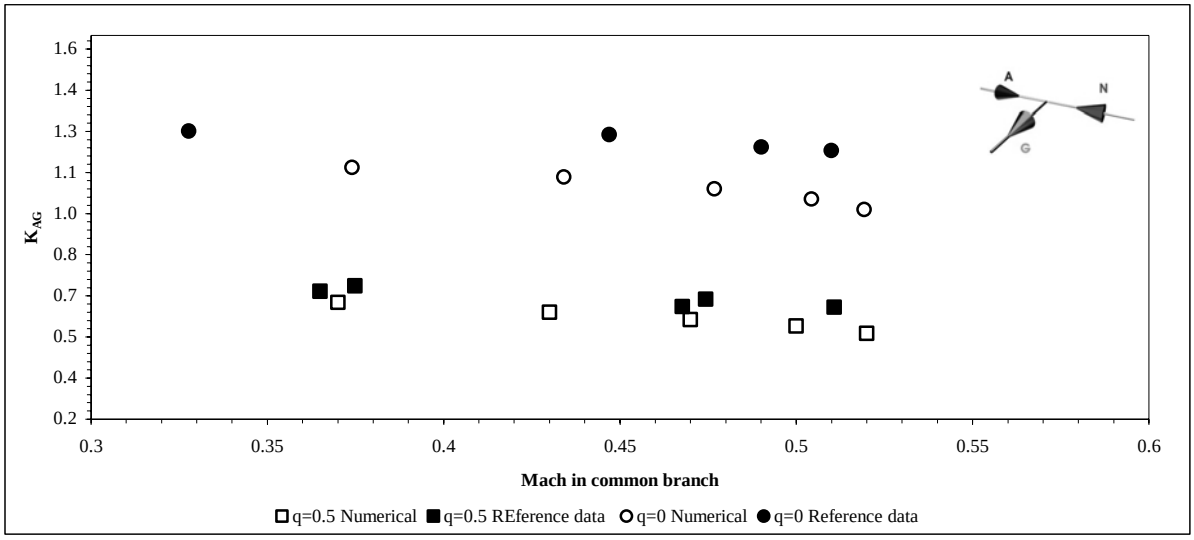

Figure 9. Coefficient K_{AG} with realizable k-ε non-equilibrium turbulence model in a V5 flow type

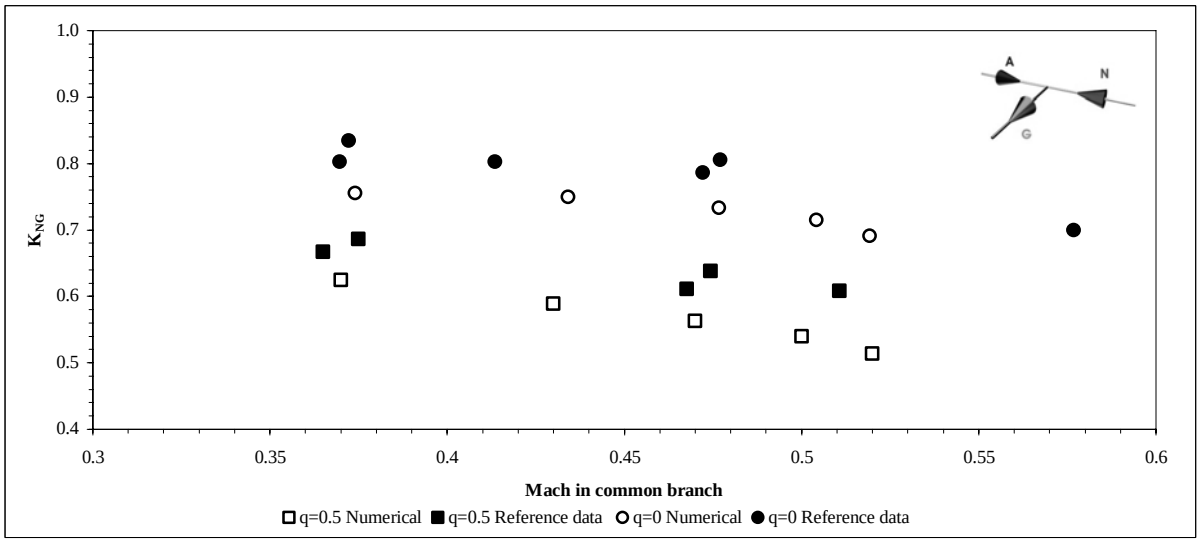

Figure 10. Coefficient K_{NG} with realizable k-ε non-equilibrium Turbulence model in a V5 flow type

.

In V5 flow type, by symmetry, only two mass flow ratio are analized. In this case a good agreement between numerical results and reference data exists for the K_{AG} y K_{NG} loss coefficients, both quantitatively, the errors are less than 5 per cent, and qualitatively, in trend.

In general, if can be observed higher coincidence at low Mach. When the number increases Mach the difference also does.

6.4.3 COMPARISON BETWEEN NUMERICAL RESULTS AND REFERENCE DATA FOR T1 FLOW TYPE

In general, in dividing cases not so good agreement between reference and numerical results are obtained. In the T1 flow type, numerical results are under or over predicted regarding the reference data. Estimated values for K_{AG} coefficient are lower than reference data. However, computed values for K_{NG} coefficient in $q = 0$ are excelent. On the other hand, for $q = 1$ and $q = 0.5$ the K_{AG} coefficient is underestimated while the K_{NG} coefficient is overstimated at low Mach number and good agreement is achieved in high Mach number.

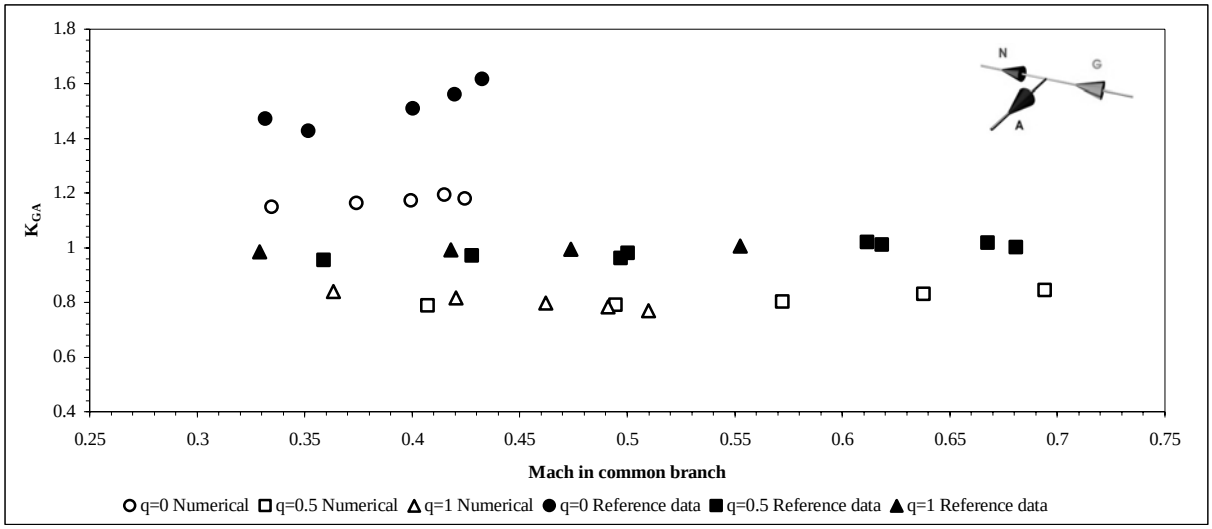

Figure 11. Coeficient K_{AG} with realizable k-ε non-equilibrium turbulence model in a T1 flow type

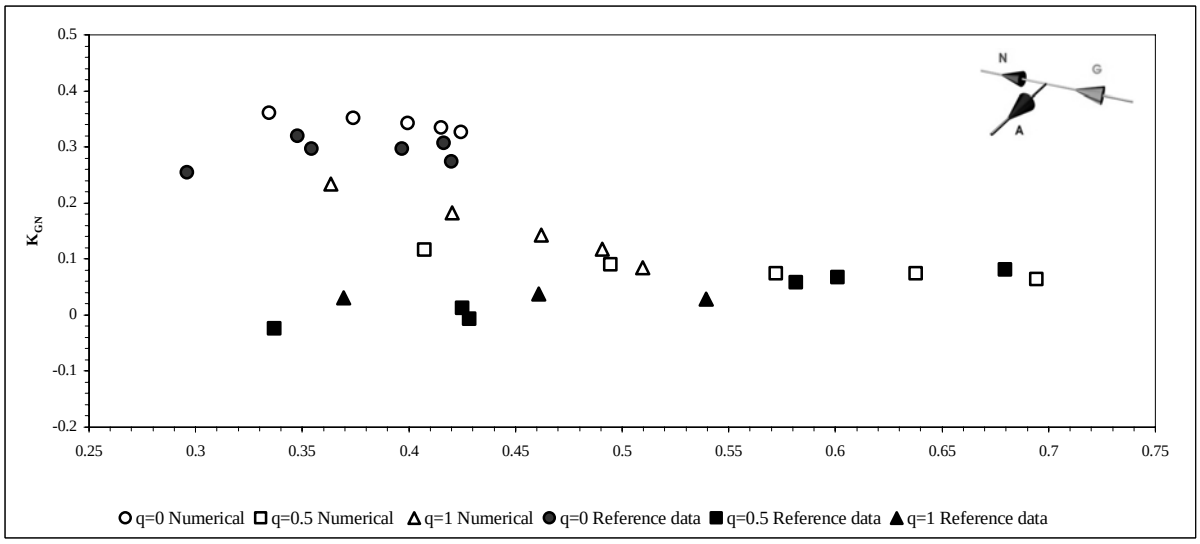

Figure 12. Coeficient K_{NG} with realizable k-ε non-equilibrium turbulence model in a T1 flow type

6.4.4 COMPARISON BETWEEN NUMERICAL RESULTS AND REFERENCE DATA FOR T2 FLOW TYPE

In general, acceptable agreement for a T2 flow type at the extreme mass flow ratios ($q = 0$ and $q = 1$) have been obtained, however, higher differeces than in the other studied flow types for mass flow ratio of $q = 0.5$ have been found. In order to improve the numerical results, several changes are been tested. So, mesh adaption and another turbulence model are been analyzed. In this way, the Spalart-Allmaras turbulence model has been applied, obtaining better results comparing with reference data.

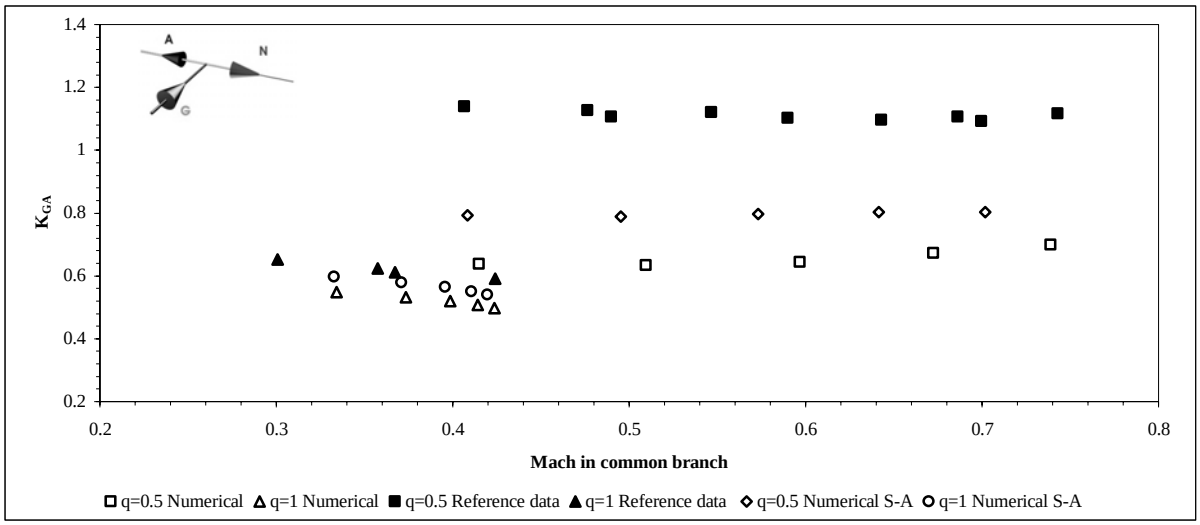

Figure 13. Coefficient K_{AG} with realizable k-ε non-equilibrium Turbulence model in a T2 flow type

.

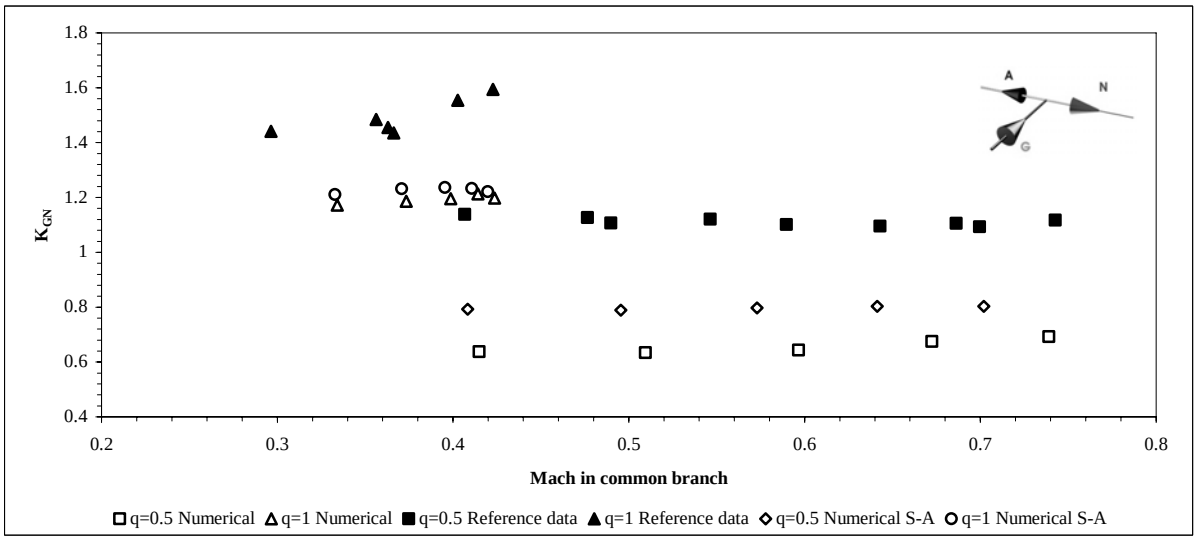

Figure 14. Coefficient K_{NG} with realizable k-ε non-equilibrium turbulence model in a T2 flow type

CONCLUSIONS

3D CFD simulations is being accomplished to computed the total pressure loss coefficients at three-way T-type junctions in subsonic compressible flow. The general purpose simulation software Fluent has been used libe a flow bench. Besides test are carried out in test rig in order to obtain empirical total pressure loss coefficient to validate the numerical procedure.

The influence of the 3D geometry definition, the adopted turbulence models as well as wall-treatment, choosed solver and other simulation parameters, such as, boundary conditions and wall roughness, has been analyzed.

The additional length of straigh pipe upstream and downstream required is $45D$ and a bevel egde in the branch intersection improve the solutions. The grid sensitivity has been studied and a y^+ interval $25 < y^+ < 100$ is obtained in all simulated cases.

The segregated solver provides accurately enough results and the computation time is much lower than coupled solver. The turbulence model which provide more feasible results in general and for differentes flow types and mass flow rates is the $k-\varepsilon$ realizable with non-equilibrium wall function. Other turbulence model like the $k-\varpi$ SST and the Spalart-Allmaras also provide adequate results in several fow types.

The “mass flow inlet” and “pressure outlet” are the most suitable boundary condition for joining flows. At dividing flow types, mass flow ratio have to be fixed by user activating the option “target-mass-flow-rate-settings” .

For a 90 deg T-junction typical in industrial fluid power pneumatic systems, the total pressure loss coefficient has been computed departing from, numerical results obtained by Fluent and measurements and experimental data measured in a flow bench.

The simulations and test have been accomplished for different flow types, mass flow rate between branches and the extrapolated Mach number in the common branch.

The pressure loss coefficient results obtained by means of simulations have been compared with own experimental data, likewise, our experimental data has been verified by comparison with other researcher’s reference data.

In general, the numerical results obtained in joining flow types and mass flow ratio 0.5 show a good agreement. However, for mass flow ratios 0 and 1 or when the coefficient is negative, worse concordance it can be observed. For the dividing flow cases, the loss coefficient relationship with Mach number is correctly predicted, although quantitatively in the most of cases are underestimated.

Finally, it is important to emphazise that the numerical simulations permit to know the internal estructure of the complex flow inside T-junction.

CONTACT

José Pérez García
Industrial Engineer
Lecturer of Department of Thermal and Fluid Engineering
Technical University of Cartagena. Spain
pepe.perez@upct.es

ACKNOWLEDGMENTS

The authors are grateful to the Seneca Foundation of Region of Murcia by support through research project PB/19/FS/97 and to the Tecnhical University of Cartagena for their continuing support of this research work.

REFERENCES

1. **Benson, R.S.**, 1975, *A simple algoritm for a multi-pipe junction in non-steady homentropic flow*, Int. Journal. Mech. Eng. Science., Vol. 17, pp. 40-41
2. **Binghan, J.F.; Blair, J.P.**, 1985, *An improved branched pipe model for multicylinder automotive engine calculation*, Proc. Inst. Mech. Eng., D1, pp. 65-77
3. **Dadone, A.**, 1973, *Perdite di carico nelle giuzinoni*, *ATA 26*, pp. 214-224
4. **Morimune, T.; Hirayama, N.; Toshiyuki Maeda, T.**, 1981, *Study of compressible high speed gas flow in piping system*, Bulletin of the JSME, Vol. I24, Nº 198, pp. 2082-20892
5. **Seifert, H.; Schindler, P.**, 1987, *New findings concerning the gas dynamic effects of manifold junctions with injector effect (pulse-converter)*, Valencia, ponencia CMT 8705
6. **Miller, D.S.**, 1971, *Internal Flow: a guide to losses in pipe and duct system*, BHRA, pp. 329
7. **Miller, D.S.**, 1978, *Internal flow systems*, BHRA Fluid Engineering, pp. 220-259
8. **Miller, D.S.**, 1984, *Compressible Internal Flow*, BHRA Fluid Engineering
9. **ESDU** Item Nº: 73022, 1973, *Pressure losses coefficients in three-leg pipe junctions: dividing flows*, ESDU International plc,. London
10. **ESDU** Item Nº: 73023, 1973, *Pressure losses coefficients in three-leg pipe junctions: combining flows*, ESDU International plc., London
11. **Ward-Smith, A.W.,** 1964, *Subsonic Adiabatic Flow in a Duct of Constant Cross-sectional Area*, Journal Royal Aeronautical Society
12. **ESDU** Item Nº: 83037, 1983, *Pressure losses coefficients in bends*, ESDU International plc., London
13. **Benedict, R.P.,** 1980, *Fundamentals of Pipe Flow*, Jhon Wiley &Sons, New York
14. **Abou-Haidar, N.I.,** 1989, Compressible flow pressure losses in branched ducts, Thesis, The University of Liverpool, Dep. Mech. Eng.
15. **Abou-Haidar, N. I.**, 1994, Compressible flow pressure losses in branched ducts. Journal of Turbomachinery, Vol. 116/537
16. **Fu, H., Tindal, M.J., Watkins, A.P., Yianneskis, M.**, 1992, *Computation of three-dimensional turbulent flows in a pipe junction with reference to engine inlet manifolds*, Proc. Instn. Mech. Engrs., Vol 206 C02192, pp. 285-296
17. **Fu, H., Watkins, A.P., Yianneskis, M.**, 1994, *The effects of flow split ratio and flow rate in manifolds*, Int. Journal for numerical methods in fluids, Vol 18, pp. 871-876
18. **Kuo, T.W., Chang, S.**, 1993, *Three-dimensional steady flow computations in manifold-type junctions and a comparison with experiment*, Paper SAE 932511
19. **Leschziner, M.A., Dimitriadis, K.P.**, 1989, *Computation of three-dimensional turbulent flow in non-orthogonal junctions by a branch-coupling method*, Computer & Fluids, Vol 17, Nº 2, pp.371-396

20. **Zhao, Y.**, Winterbone, D.E., 1994, *A study of multi-dimensional gas flow in engine manifolds*, Proc. Inst. Mech. Eng., Vol 218, Part C, D04892
21. **Shaw, C.T., Lee, D.J., Richarson, S.H., Pierson, S.**, 2000, *Modelling the effect of plenum-runner interface geometry on the flow through an inlet system*, Paper SAE 2000-01-0569
22. **Pan, W., Cui, Y., Leylek, J.H., Sommer, R.G., Jair, S.K.**, 1999, *A CFD study of losses in a straight-six diesel engine*, Paper SAE 1999-01-0230
23. **Taylor, W., Leylek, J.H., Tran, L.T., Shinogle, R.D., Jain, S.K.**, 1997, *Advanced computational methods for predicting flow losses in intake regions of diesel engines*, paper SAE 970639
24. **Zucrow, M.J.; Hoffman, J.D.**: *Steady one-dimensional flow with friction*. John Wiley & Sons, *Gas Dynamics (I) Chapter 5*, 1ª edition. New York, 1976, "242-326" pp
25. **J. Pérez García, J. Hernández Grau, J. Martínez García, A. Cano Cerón, A. Sánchez Kaiser y A. Viedma Robles**., 2002, Determinación mediante simulación numérica del coeficiente de fricción en tubo recto de sección constante para flujo compresible, adiabático y estacionario. Validación experimental**.** Fluent users meeting.
26. http://wolfram.com
27. **J. Pérez García, J. Hernández Grau, J. Martínez García A. Cano Cerón y A. Viedma Robles.**, 2002, *Desarrollo de un Banco de Flujo compresible. Aplicación a la determinación de coeficientes de pérdidas en uniones de conductos en flujo compresible estacionario.* Congreso Nacional de Ingeniería Mecánica
28. Guide to the Expression of Uncertainty in Measurement, ISO, 1993